AMSE JOURNALS-AMSE IIETA publication-2017-Series: Modelling A; Vol. 90; N°2; pp 240-255
Submitted Apr. 09, 2017; Revised Jun. 08, 2017; Accepted Jun. 20, 2017

Pentaprism Measurements of Large Flat Mirrors

*Li Yuan, **Xiaohui Zhang, ***Xu He

*Changchun Institute of Optics, Fine Mechanics and Physics, Chinese Academy of Sciences, Changchun 130033, China; University of Chinese Academy of Sciences, Beijing 100049, China
**Changchun Institute of Optics, Fine Mechanics and Physics, Chinese Academy of Sciences, Changchun 130033, China (xhz861@outlook.com)
***Changchun Institute of Optics, Fine Mechanics and Physics, Chinese Academy of Sciences, Changchun 130033, China

Abstract

In view of the difficulty in measuring large flat mirrors, this paper introduces a pentaprism system that measures the angle differences between points on the mirror surface with a scanning pentaprism. Based on the angle differences, many equations were established and the mirror surface was expressed through a least squares calculation. The error analysis reveals that the system accuracy was 11.6nm root-mean-square (rms) over a 1.5m flat mirror. Then, the pentaprism measurement was compared with Ritchey-Common test. The comparison shows that the difference between the two results is 10.2nm rms over a 1.5m flat mirror, which is within the error range of the pentaprism system. Thus, the proposed pentaprism system is applicable to the measurement of large flat mirrors.

Keywords

Pentaprism, Large flat mirror, Tilt angle, Angle difference, Least squares calculation.

1. Introduction

Following the conventional interferometry technique, it is impractical to measure large flat mirrors with an aperture greater than 1m. m The largest aperture of commercial interferometers is about 900mm, which is insufficient to cover the entire surface of a said large flat mirror. To overcome the problem, two methods have been developed, namely sub-aperture stitching

interferometry [1,2] and Ritchey-Common test [3-5]. However, the accuracy and efficiency of the sub-aperture stitching interferometry are not high when the sub-apertures are far smaller than the test mirror. The Ritchey-Common test can measure the full surface of a large flat mirror, only if there is a reference spherical mirror even larger than the test mirror. Sometimes, it is impossible to obtain such a reference mirror. The introduction of a pentaprism system may make up for the defects of the current methods.

A range of pentaprism systems have been developed to measure large optical surfaces. Such systems can be roughly divided into two types. The first type of pentaprism system contains one scanning pentaprism that directly measures the tilt angles on the surface [6-12]. This system is sensitive to errors, such as the tilt of the autocollimator, the manufacturing errors of the pentaprism, and the environmental influence. The second type consists of two pentaprisms, a stationary reference pentaprism and a scanning pentaprism, that measure the angle differences between points on the test surface [13-16]. This system eliminates the first-order errors caused by tilt, and most of the environmental influence. However, it fails to offset the inevitable manufacturing errors of the two pentaprisms in the calculation of angle differences.

In this research, a novel pentaprism system is proposed to measure large flat mirrors with an aperture no greater than 2m. The proposed system was improved in four aspects from the above-mentioned two types of systems. First, the angle differences are measured by only one scanning pentaprism to eliminate the first-order errors caused by tilt, most of the environmental influence, and the manufacturing errors of the two-pentaprism system. Second, the system can automatically monitor and reduce the tilt of the pentaprism. Third, the measured results are of high accuracy, for the mirror surface is expressed by Zernike polynomials and the expression is derived through a least squares calculation. Fourth, the system directly obtains the 2D surface profile without obtaining and stitching the 1D surface profiles. These improvements can improve the accuracy and efficiency of the pentaprism measurement.

2. Principles of the Measurement

A pentaprism is a five-sided reflecting prism used to deviate a beam of light by 90 degrees. The deviation angle hardly changes when the pentaprism rotates by small amounts. Figure 1 shows the light path of the measurement. The collimated beam is deflected by the pentaprism from the autocollimator to the mirror surface, and then reflected by the surface back to the autocollimator. The angle between the returning and exiting beams reveals the tilt angle on the mirror surface.

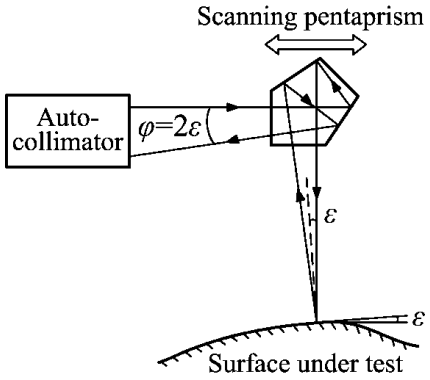

Fig.1. The Light Path of the Measurement

The autocollimator can measure both the angle along the scan direction (hereinafter referred to as the in-scan angle) and the angle perpendicular to the scan direction (the cross-scan angle). The tilt of the pentaprism only causes second-order errors to the in-scan angle, but first-order errors to the cross-scan angle. Therefore, only the in-scan angle was selected for the measurement.

Let us denote the in-scan angle obtained by the autocollimator as φ (Figure 1). Then, the in-scan tilt angle ε on the mirror surface can be expressed as

$$\varepsilon = \frac{\varphi}{2}. \tag{1}$$

When the pentaprism is scanning on the rails, it is possible to acquire the tilt angles of many points on the mirror surface. If the tilt angles of any two points are ε_1 and ε_2, the angle difference δ between the two points can be derived as

$$\delta = \varepsilon_2 - \varepsilon_1. \tag{2}$$

Many common errors can be eliminated by calculating the angle difference. For example, if the autocollimator has a tilt angle ω (Figure 2), the angle obtained by the autocollimator is $\varphi = 2(\varepsilon+\omega)$. Whereas the tilt angle ω does not change during the scanning, the angle difference δ between the two points is

$$\delta = \frac{\varphi_2}{2} - \frac{\varphi_1}{2} = (\varepsilon_2 + \omega) - (\varepsilon_1 + \omega) = \varepsilon_2 - \varepsilon_1. \tag{3}$$

The result of Equation (3) is the same as that of Equation (2), indicating that the error ω has no impact on the angle difference.

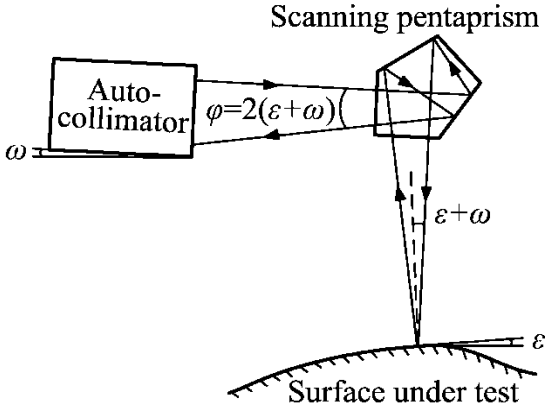

Fig.2. Elimination of Tilt Angle ω

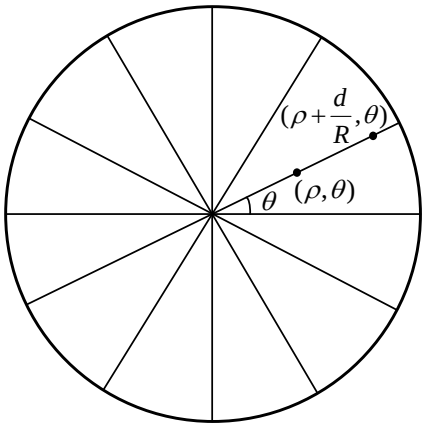

Fig.3. Six radial Scans through the Mirror Centre

Six radial scans were carried out through the mirror centre (Figure 3). Every two adjacent scans were separated by 30° . In the cylindrical coordinate system, the mirror surface $S(\rho,\theta)$is expressed by Zernike polynomials $Z_i(\rho,\theta)$ as follows:

$$S(\rho,\theta)=\sum_{i=1}^{n}C_iZ_i(\rho,\theta), \tag{4}$$

where ρ is the normalized radial distance ($0\le\rho\le1$); θ is the normalized azimuthal angle ($0\le\theta<2\pi$); C_i are the Zernike coefficients; n is the number of Zernike polynomials. Let d be the distance between the two points, R be the radius of the test mirror, and (ρ,θ) and $(\rho+d/R,\theta)$ be the normalized coordinates of the two points (Figure 3). The angle ε is so small that is equals the

derivative of $S(\rho,\theta)$ versus ρ. Then, the following equations hold:

$$\varepsilon_1 = \frac{1}{R}\frac{\partial S(\rho,\theta)}{\partial \rho} = \frac{1}{R}\sum_{i=1}^{n} C_i \frac{\partial Z_i(\rho,\theta)}{\partial \rho}, \tag{5}$$

$$\varepsilon_2 = \frac{1}{R}\frac{\partial S(\rho+\frac{d}{R},\theta)}{\partial \rho} = \frac{1}{R}\sum_{i=1}^{n} C_i \frac{\partial Z_i(\rho+\frac{d}{R},\theta)}{\partial \rho}. \tag{6}$$

When the radial distance is divided by R to be normalized to $\rho(0\leq\rho\leq1)$, the tilt on the surface is multiplied by R. Hence, the right sides of Equations (5) and (6) must be divided by R. The following equation can be obtained by subtracting Equation (5) from Equation (6).

$$\delta = \frac{1}{R}\sum_{i=1}^{n} C_i \left[\frac{\partial Z_i(\rho+\frac{d}{R},\theta)}{\partial \rho} - \frac{\partial Z_i(\rho,\theta)}{\partial \rho} \right]. \tag{7}$$

where C_i are the only unknown variables. Based on Equation (7), it is possible to derive the equations of various pairs of points. Then, C_i can be obtained through a least squares calculation, and the expression of the mirror surface can be derived as Equation (4).

Note:

(1). The two points must be in the same scan and share the same azimuthal angle.

(2). The distance d between the two points must exceed 200mm, because small distance narrows down angle difference and magnifies relative errors.

(3). The two points must be measured quickly one after the other to minimize the influence of environmental changes.

3. Control of Pentaprism Tilt

Owing to the imperfectness of the rails, the pentaprism will tilt inevitably during scanning. Hence, an autocollimator and a return mirror were added to monitor the tilt. As shown in Figure 4, Autocollimator 1 is mainly used to measure the mirror surface, while Autocollimator 2 and the return mirror are used to monitor the pentaprism tilt. The return mirror and the pentaprism are installed on the same mount.

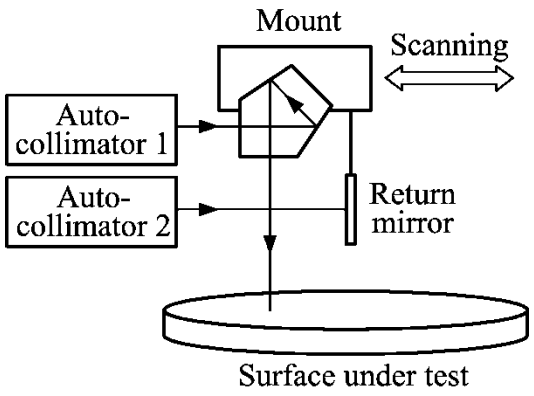

Fig.4. Autocollimator 2 and Return Mirror

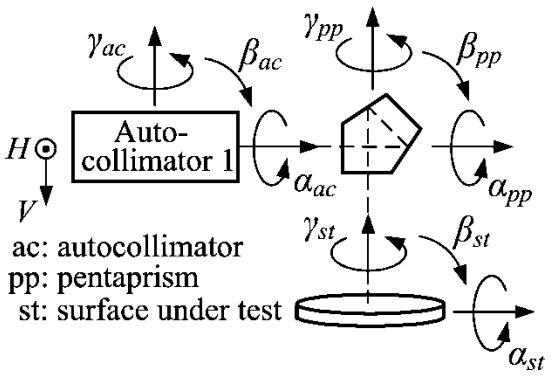

Fig.5. Tilt Angles of Optical Components

The tilt angles of the optical components are defined in Figure 5. Let us denote V as half of the in-scan angle obtained by Autocollimator 1 and H as half of the cross-scan angle. Actually, V is the tilt angle ε in Equation (1) with some errors. Through ray tracing calculations, V and H can be derived as[17].

$$V = -\alpha_{pp}{}^2 + \alpha_{ac}(\alpha_{pp} - \gamma_{pp} - \alpha_{st}) + \alpha_{st}(\alpha_{pp} + \gamma_{pp}) - \beta_{st} + \beta_{ac} + V_0, \tag{8}$$

$$H = \beta_{st}(\alpha_{pp} + \gamma_{pp} - \gamma_{st} - \alpha_{ac}) + \alpha_{st} - \alpha_{pp} + \gamma_{pp} - \gamma_{ac} + H_0, \tag{9}$$

where V_0 and H_0 are constant angles resulted from the manufacturing errors of the pentaprism. If Δ is used to indicate the change from the pre-scan value, then the change ΔH can be derived as below without considering the second-order terms in Equation (9):

$$\Delta H = \Delta\alpha_{st} - \Delta\alpha_{pp} + \Delta\gamma_{pp} - \Delta\gamma_{ac} + \Delta H_0, \tag{10}$$

where $\Delta\gamma_{ac}$= 0 for Autocollimator 1 is stationary in each scan; ΔH_0= 0 as H_0 is a constant value; on the polished mirror surface, $\Delta\alpha_{st}$ is about 3μrad rms, and $\Delta\alpha_{pp}$ and $\Delta\gamma_{pp}$ are both about 50μrad rms. $\Delta\alpha_{st}$ is negligible for it is much smaller than $\Delta\alpha_{pp}$ and $\Delta\gamma_{pp}$. Then, $\Delta\alpha_{pp}$ can be derived as

$$\Delta\alpha_{pp} = \Delta\gamma_{pp} - \Delta H, \tag{11}$$

where $\Delta\gamma_{pp}$ is monitored by Autocollimator 2 and ΔH is monitored by Autocollimator 1. After the pentaprism tilts $\Delta\alpha_{pp}$ and $\Delta\gamma_{pp}$ are derived, the two parameters will be automatically adjusted to <15μrad rms through feedbacks. The monitoring and adjustment must be done prior to measurement at every test point on the mirror surface. Note that $\Delta\beta_{pp}$ has no influence on the measurement, and does not need to be controlled.

4. The Pentaprism System

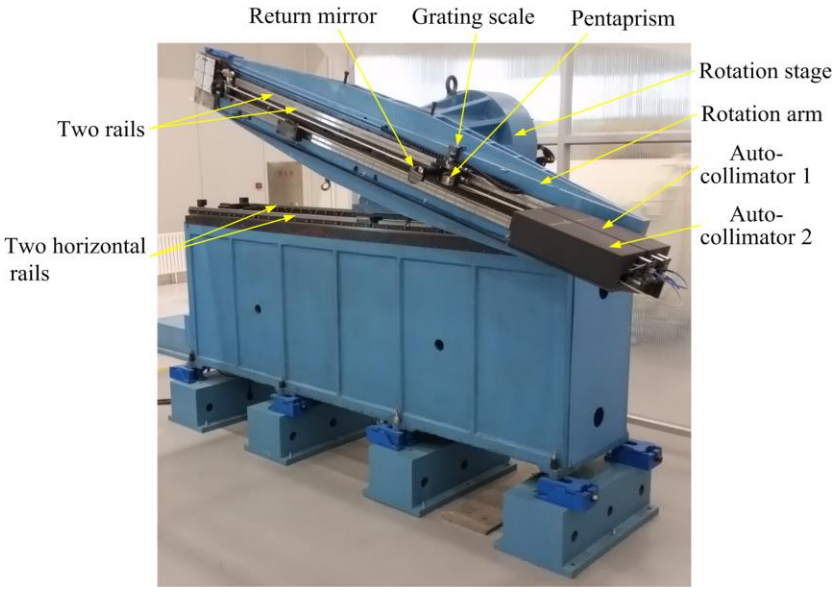

Fig.6. The Pentaprism System

The pentaprism system is illustrated in Figure 6. The pentaprism and the return mirror are fixed onto the same mount, which remotely adjusts their tilt. The mount can slide on a pair of 2.2m parallel rails along the lines of sight of the two autocollimators. During the sliding process, the tilt of the mount varies in a range of 50μrad rms. The positions of the scanning pentaprism are measured by a grating scale with an accuracy of 0.005mm rms. Autocollimator 1 (SH-LTP/Imagine Optic) emits a 27mm collimated beam, reaches an accuracy of 130nrad rms in rotation, and boasts a full measurement range of ±12mrad. Autocollimator 2 is exactly the same as Autocollimator 1. All the components mentioned above are fixed onto a rotation arm. The arm,

mounted on a rotation stage (rotation angle error: 75μrad rms), can rotate for multiple scans. During the rotation process, the tilt of the arm varies in a range of 70μrad rms.

As stated by Geckeler [17], the initial system alignment should be conducted in reference to Autocollimator 1. After the alignment, the initial tilt of all the optical components must be less than 10μrad rms.

5. Error Analysis

5.1 Tilt Errors

From Equations (8) and (9), it can be seen that α_{pp} and γ_{pp} cause second-order errors to V and first-order errors to H. Thus, only V should be adopted for the measurement.

Let us assume that the two points are Point 1 and Point 2, and the change from Point 1 to Point 2 is Δ. It should be noted that the Δ here is different from that in Section 3. In essence, the change ΔV is the angle difference δ in Equation (2) with some errors. From Equation (8), ΔV can be derived as

$$\Delta V = \Delta\alpha_{pp}(-2\alpha_{pp} + \alpha_{ac} + \alpha_{st}) + \Delta\gamma_{pp}(-\alpha_{ac} + \alpha_{st}) + \Delta\alpha_{ac}(\alpha_{pp} - \gamma_{pp} - \alpha_{st}) + \Delta\alpha_{st}(-\alpha_{ac} + \alpha_{pp} + \gamma_{pp}) - \Delta\beta_{st} + \Delta\beta_{ac} + \Delta V_0, \quad (12)$$

where $\Delta\alpha_{ac} = \Delta\beta_{ac} = 0$ for Autocollimator 1 is stationary in each scan; $\Delta V_0 = 0$ as V_0 is a constant value. Whereas $(-\Delta\beta_{st})$ is actually the angle difference δ to be measured, the error of the angle difference δ is

$$E_\delta = \Delta\alpha_{pp}(-2\alpha_{pp} + \alpha_{ac} + \alpha_{st}) + \Delta\gamma_{pp}(-\alpha_{ac} + \alpha_{st}) + \Delta\alpha_{st}(-\alpha_{ac} + \alpha_{pp} + \gamma_{pp}). \quad (13)$$

According to Equation (13), the first-order errors in V are eliminated after calculating the angle difference, and only the second-order errors remain.

The values of some tilt angles are listed in Table 1. The author measured the root-mean-square (rms) errors of $\Delta\alpha_{pp}$, $\Delta\gamma_{pp}$ and $\Delta\alpha_{st}$, and the limit errors of other angles. The limit error is 3 times the corresponding rms error.

The calculated results of E_δ are listed in Tables 2 and 3. All the minus signs in Equation (13) were changed to plus signs to analyse errors. Note that limit errors are considered to be constant in Table 3. It is calculated that the error of the angle difference δ is 11.1nrad rms.

Tab.1. The Values of Some Tilt Angles.

Tilt angles	From initial alignment	From tilts of scanning pentaprism	From tilts of rotation arm	From local tilts in mirror surface	Root-sum-square
α_{pp}	<30 μrad	<45 μrad	<210 μrad	—	<217 μrad
$\Delta\alpha_{pp}$	—	21 μrad rms	—	—	21 μrad rms
γ_{pp}	<30 μrad	<45 μrad	—	—	<54 μrad
$\Delta\gamma_{pp}$	—	21 μrad rms	—	—	21 μrad rms
α_{st}	<30 μrad	—	—	<9 μrad	<31 μrad
$\Delta\alpha_{st}$	—	—	—	3 μrad rms	3 μrad rms
α_{ac}	—	—	<210 μrad	—	<210 μrad
β_{ac}	—	—	<210 μrad	—	<210 μrad
γ_{ac}	—	—	—	—	—

Note:

1. Since Autocollimator 1 the reference for the alignment, α_{ac}, β_{ac} and γ_{ac} have no component resulted from the initial alignment;

2.Since the γ tilt of the rotation arm is essentially the rotation angle error of the rotation stage, γ_{pp} and γ_{ac} have no component resulted from the tilt of the rotation arm (Section 5.3);

3. γ_{ac} equals 0.

Tab.2. Calculations of Some Components in Equation (13) (μrad).

Components in Eq. (13)	α_{pp}	$2\alpha_{pp}$	α_{ac}	α_{st}	γ_{pp}	Root-sum-square
$2\alpha_{pp}+\alpha_{ac}+\alpha_{st}$	—	<434	<210	<31	—	<483
$\alpha_{ac}+\alpha_{st}$	—	—	<210	<31	—	<212
$\alpha_{ac}+\alpha_{pp}+\gamma_{pp}$	<217	—	<210	—	<54	<307

Tab.3. Calculations of E_δ in Equation (13).

Terms in Eq. (13)	Values (nradrms)
$\Delta\alpha_{pp}(2\alpha_{pp}+\alpha_{ac}+\alpha_{st})$	10.1
$\Delta\gamma_{pp}(\alpha_{ac}+\alpha_{st})$	4.5
$\Delta\alpha_{st}(\alpha_{ac}+\alpha_{pp}+\gamma_{pp})$	0.9
Root-sum-square	11.1

5.2 Measurement Error of Autocollimator 1

The measurement error of Autocollimator 1 is 130nrad rms. According to Equations (1) and (2), the error of the angle difference δ can be calculated as

$$\sqrt{\left(\frac{130}{2}\right)^2+\left(\frac{130}{2}\right)^2}=91.9\ \text{nrad rms.} \tag{14}$$

5.3 Position Errors of Measurement Points

The rotation angle error of the rotation stage is 75μrad rms, and the radius of the mirror is assumed to be 750mm, so the corresponding position error is less than

$$75\times10^{-6}\times750=0.056\,\text{mm rms.} \tag{15}$$

The position error from the scan of the pentaprism is 0.005mm rms, which is the accuracy of the grating scale.

The angles α_{pp}, γ_{pp}, β_{ac}, γ_{ac}, V_0 and H_0, the first-order terms in Equations (8) and (9) except $\alpha_{st}$and β_{st}, refer to the tilt angles of the beams towards the mirror. The corresponding position errors equal the products of the beam tilt angles and the distance between the pentaprism and the mirror (Table 4).

Tab.4. Calculations of the Position Errors Corresponding to Beam Tilt Angles.

Beamtilt angles (μradrms)	Distance between pentaprism and mirror (mm)	Position errors (mm rms)
From α_{pp}: 72	500	0.036
From γ_{pp}: 18	500	0.009
From β_{ac}: 70	500	0.035
From V_0: 16	500	0.008
From H_0: 16	500	0.008
Root-sum-square		0.052

Note:

(1).The values of α_{pp}, γ_{pp} and β_{ac} are the same as those in Table 1;

(2). γ_{ac} is excluded because it equals 0.

The three kinds of position errors are combined into:

$$\sqrt{0.056^2+0.005^2+0.052^2}=0.077\,\text{mm rms.} \tag{16}$$

The position error 0.077mm rms has a minor influence on the flat and polished test surface. It is estimated that the tilt angle ε changes by less than 15nrad/mm on the mirror surface. Thus, the error of tilt angle ε is 1.2nrad rms. According to Equation (2), the error of the angle difference δ is 1.7nrad rms.

5.4 Manufacturing Errors of the Pentaprism

The manufacturing errors of the pentaprism is the root cause of the constant angle errors V_0

and H_0 (Equations (8) and (9)), which have been analysed in Sections 5.1 and 5.3. It can be seen from Equation (13) that V_0 is eliminated in the calculation of angle difference.

5.5 Errors from Environmental Changes

To reduce environmental changes, the system and the test mirror were placed on a vibration isolation platform at the ambient temperature of 20°C±0.2°C without the movements of people and other things.

Assuming that two matching points are separated by 300mm, it only takes 15sec for the pentaprism to measure the two points. Within such a short period of time, the environmental changes are so small as to be negligible in the calculation of angle difference.

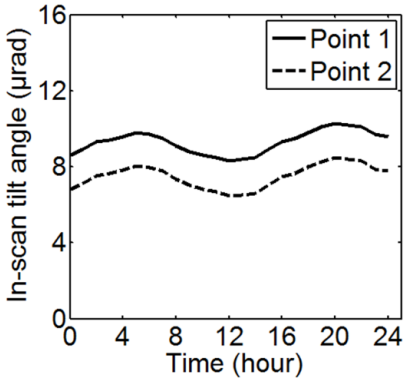

Fig.7. The In-scan Tilt Angles of the Two Fixed Points

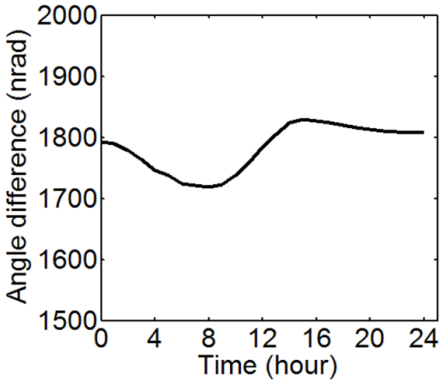

Fig.8. The Angle Difference between the Two in-scan Tilt Angles

Two fixed points, separated by 300mm, were selected on the mirror surface. The angle difference between them was measures once every 10mins for 24h. The obtained in-scan tilt angles of the two fixed points are illustrated in Figure 7, and difference between the two angles is displayed in Figure 8. As shown in Figure 7, the two tilt angles shared the same variation trend.

The standard deviations of the tilt angles of Points 1 and 2 were 607.6nrad and 620.2nrad respectively, and the standard deviation of the angle difference was merely 38.5nrad.

5.6 Combined Error

The combined error of the angle difference is 100.3nrad rms (Table 5).

Tab.5. Calculations of the Combined Error of the Angle Difference.

Error sources	Errors (nrad rms)
Tilt errors	11.1
Measurement error of Autocollimator 1	91.9
Position errors	1.7
Errors from changing environment	38.5
Root-sum-square	100.3

5.7 Monte Carlo Simulation

The angle difference errors and their effects on the obtained surface profile were simulated on MATLAB by Monte Carlo method. The object is a 1.5m flat mirror with 20 pairs of measurement points per azimuthal angle. Every two matching points were separated by 300mm. The measurement contained a total of 6 scans. With the aid of MATLAB, the angle differences were generated for all the pairs of points and the random error of 100.3nrad rms was produced for all the angle differences. Two surface profiles were calculated, respectively using the angle differences with and without these errors. The difference between the two surface profiles is called the profile error. The rms value of the profile errors is 11.6nm, which reflects the error range of our system.

6. Measurement Results and Comparison

As mentioned above, our system was used to measure a 1.5m flat mirror (Figure 9). The measurement involved six scans and 20 pairs of measurement points per azimuthal angle. The distance between every two matching points was 300mm. Eight primary Zernike polynomials were chosen to express the mirror surface. The mirror was measured 10 times under the same conditions. The standard deviations of the 10 profile results are shown in Figure 10. The largest standard deviation (9.3nm) only occurred on the edge of the mirror, and the standard deviations was averaged at 6.8nm, signifying the repeatability of the system. The average Zernike coefficients are listed in Table 6. The average surface map is shown in Figure 11.

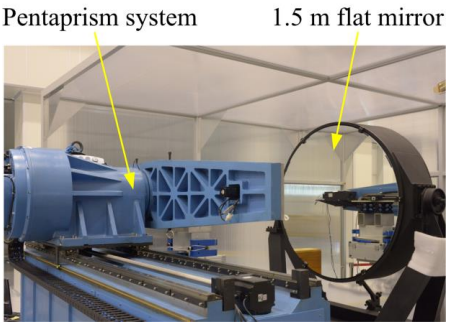

Fig.9. Simulation

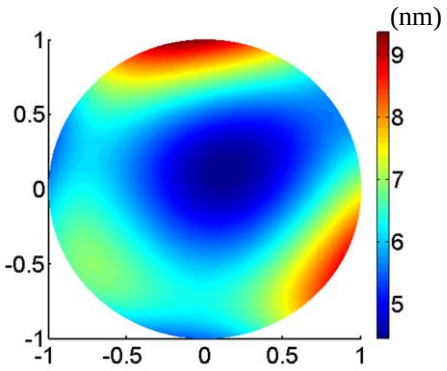

Fig.10. The Standard Deviations of the 10 Profile Results

Tab.6. The Average Zernike Coefficients from the Pentaprism Measurements.

Zernike polynomials	Zernike coefficients(nm)
Power: $Z_4= 2\rho^2-1$	37.1
Cosine astigmatism: $Z_5= \rho^2\cos2\theta$	-42.6
Sine astigmatism: $Z_6=\rho^2\sin2\theta$	19.9
Cosine coma: $Z_7= (3\rho^2-2)\rho\cos\theta$	43.0
Sine coma: $Z_8= (3\rho^2-2)\rho\sin\theta$	39.5
Spherical: $Z_9= 6\rho^4-6\rho^2+1$	-25.3
Cosine trefoil: $Z_{10}= \rho^3\cos3\theta$	10.4
Sine trefoil: $Z_{11}= \rho^3\sin3\theta$	-7.8

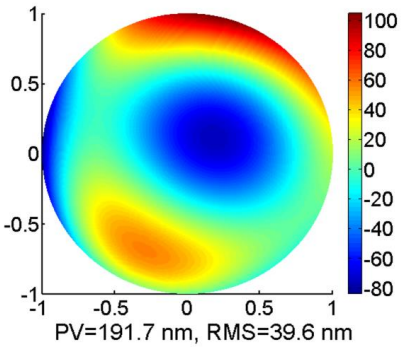

Fig.11. The Average Surface Map from the Pentaprism Measurements

For comparison, another method, the Ritchey-Common testing, was introduced to measure the 1.5m flat mirror [3-5]. As shown in Figure 12, the test device consists of an interferometer, the 1.5m flat mirror, and a 1.8m spherical mirror. The obtained surface map is shown in Figure 13.

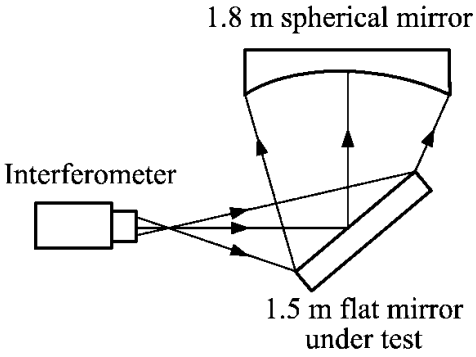

Fig.12. The Configuration of Ritchey-Common Test Device

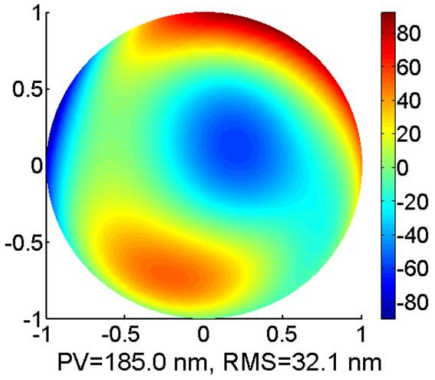

Fig.13. The Surface Map from Ritchey-Common Test

Through the comparison between Figures 11 and 13, it can be seen that the two methods yielded almost the same results. The rms value of the difference between the two surface maps was 10.2nm, which fell within the error range (Section 5.7) of the pentaprism system.

Conclusions

This paper introduces a novel pentaprism system to measure large flat mirrors with an aperture no greater than 2m. The system that measures the angle differences between points on the mirror surface with a scanning pentaprism, and derives the expression of the mirror surface through a least squares calculation.

It is discovered that the system can effectively reduce various errors. First, the first-order

errors caused by tilt were eliminated by the error-reducing property of the pentaprism and the calculation of the angle differences. Second, the second-order errors caused by tilt were reduced by the control of the pentaprism tilt. Third, the effect of the manufacturing errors of the pentaprism was ameliorated by the calculation of the angle differences. Fourth, the relative errors were offset by the long spacing between the two matching points. Fifth, the environmental influence was removed by the the calculation of the angle differences, the strict control of environment and the short time between the measurements of the two matching points.

Through the error analysis, it is concluded that the proposed system has an error range of 11.6nm rms over a 1.5m flat mirror. The pentaprism measurement was then contrasted with Ritchey-Common test. The resulting difference was 10.2nm rms over a 1.5m flat mirror, which fell within the error range of the pentaprism system. Thus, the proposed pentaprism system is applicable to the measurement of large flat mirrors.

Acknowledgments

This work was supported by National Natural Science Foundation of China (Grant Nos. 61675198 and 61307114).

References

1. S. Chen, S. Xue, Y. Dai, S. Li, Subaperture stitching test of large steep convex spheres, 2015, Optics Express, vol. 23, no. 22, pp. 29047-29058.
2. H. Chang, C. Liang, P. Lin, Y. Chen, Measurement improvement by high overlapping density subaperture stitching interferometry, 2014, Applied Optics, vol. 53, no. 29, pp. H102-H108.
3. S. Zhu, X. Zhang, Eliminating alignment error and analyzing Ritchey angle accuracy in Ritchey–Common test, 2013, Optics Communications, vol. 311, pp. 368-374.
4. B. Ji, C. Xu, B. Li, The error analyze of testing the large aperture flat by the Ritchey-Common method, 2014, Proc. SPIE, vol. 9298, pp. 92981A.
5. S. Zhu, X.H. Zhang, Application of error detaching to Ritchey-Common test for flat mirrors, 2014, Optics and Precision Engineering, vol. 22, no. 1, pp. 7-12.
6. J.L. Pearson, G.W. Roberts, P.C.T. Rees, S.J. Thompson, Use of a NOM profilometer to measure large aspheric surfaces, 2015, Proc. SPIE, vol. 9628, pp. 96280W.
7. R.D. Geckeler, N.A. Artemiev, S.K. Barber, A. Just, I. Lacey, O. Kranz, B. V. Smith, V.V. Yashchuk, Aperture alignment in autocollimator-based deflectometricprofilometers, 2016, Rev. Sci. Instrum., vol. 87, pp. 051906.
8. S.K. Barber, R.D. Geckeler, V.V. Yashchuk, M.V. Gubarev, J. Buchheim, F. Siewert, T.

Zeschke, Optimal alignment of mirror-based pentaprisms for scanning deflectometric devices, 2011, Optical Engineering, vol. 50, no. 7, pp. 073602.

9. S. Qian, L. Wayne, M. Idir, Nano-accuracy measurements and the surface profiler by use of Monolithic Hollow Penta-Prism for precision mirror testing, 2014, Nuclear Instruments and Methods in Physics Research A, vol. 759, pp. 36-43.
10. S.K. Barber, G.Y. Morrison, V.V. Yashchuk, M.V. Gubarev, R.D. Geckeler, J. Buchheim, F. Siewert, T. Zeschke, Developmental long-trace profiler using optimally aligned mirror-based pentaprism, 2011, Optical Engineering, vol. 50, no. 5, pp. 053601.
11. F. Siewert, T. Zeschke, T. Arnold, H. Paetzelt, V.V. Yashchuk, Linear chirped slope profile for spatial calibration in slope measuring deflectometry, 2016, Rev. Sci. Instrum., vol. 87, pp. 051907.
12. J. Qian, J. Sullivan, M. Erdmann, A. Khounsary, L. Assoufid, Performance of the APS optical slope measuring system, 2013, Nuclear Instruments and Methods in Physics Research A, vol. 710, pp. 48-51.
13. P.C.V. Mallik, C. Zhao, J.H. Burge, Measurement of a 2-meter flat using a pentaprism scanning system, 2007, Optical Engineering, vol. 46, no. 2, pp. 023602.
14. E. Qi, H. Hu, H. Hu, G. Cole, X. Luo, V. Ford, X . Zhang, The application of pentaprism scanning technology on the manufacturing of M3MP, 2016, Proc. SPIE, vol. 9682, pp. 96821A.
15. J. Yellowhair, J.H. Burge, Analysis of a scanning pentaprism system for measurements of large flat mirrors, 2007, Applied Optics, vol. 46, no. 35, pp. 8466-8474.
16. R. Allen, P. Su, J.H. Burge, B. Cuerden, H.M. Martin, Scanning pentaprism test for the GMT 8.4 m off-axis segments, 2010, Proc. SPIE, vol. 7739, pp. 773911.
17. R.D. Geckeler, Optimal use of pentaprisms in highly accurate deflectometric scanning, 2007, Meas. Sci. Technol., vol. 18, pp. 115-125.